ISSN 1807-1929
Revista Brasileira de Engenharia Agrícola e Ambiental
Brazilian Journal of Agricultural and Environmental Engineering
v.30, n.9, e304015, 2026
Campina Grande, PB – http://www.agriambi.com.br – http://www.scielo.br/rbeaa

DOI: https://doi.org/10.1590/1807-1929/agriambi.v30n9e304015 ORIGINAL ARTICLE

# Development of floating waterwheel-driven pumping system for rural use[1]

## Desenvolvimento de sistema de bombeamento por roda d'água flutuante para uso rural

Marcelo P. Rotta[2*], Carlos E. C. Nogueira[2], Jair A. C. Siqueira[2], Eloy L. de Mello[2], Marcio A. Vilas Boas[2] & Samuel N. M. de Souza[2]

[1] Research developed at Universidade Estadual do Oeste do Paraná, Cascavel, PR, Brazil
[2] Universidade Estadual do Oeste do Paraná, Campus de Cascavel, PR, Brazil

*HIGHLIGHTS:*

*The floating system pumped water without electricity or fuel.*
*Flow rates met the daily water demand of small rural properties.*
*Simple construction favored low cost and suitability for off-grid rural applications.*

**ABSTRACT:** Access to water for irrigation and agricultural activities in remote rural areas often depends on alternative energy solutions, especially in locations without connection to the electric power grid. This study proposes to construct and experimentally evaluate a pumping system driven by a floating water wheel, designed to operate continuously in rivers with moderate flow, presenting itself as a sustainable, low-cost alternative suited to the needs of family farmers and rural communities. The system was constructed, installed, and tested along a stretch of the Tormenta River, in the municipality of Catanduvas, in the state of Paraná, Brazil, where measurements of pumped flow rate, manometric head, torque, rotational speed, and current velocity were performed. Based on experimental data, hydraulic power, mechanical power, and pumping power were determined, as well as the hydraulic, mechanical, and overall efficiencies of the system. The prototype operated continuously, despite the intermittent behavior characteristic of the Wirtz pump, and achieved a maximum hydraulic efficiency of 72%. The pumped flow rates proved to be compatible with the water demands of small family-owned agricultural properties. The economic analysis indicated that the system is viable when compared to the avoided cost of conventional water supply, presenting a discounted payback period shorter than the estimated service life of the equipment and a levelized cost of energy close to one Brazilian real per cubic meter of pumped water. The results demonstrate that floating water wheels constitute a sustainable, low-cost, and technically feasible solution for isolated rural communities.

**Key words:** hydrokinetic energy, water lifting, autonomous water supply, alternative irrigation, renewable water supply

**RESUMO:** O acesso à água para irrigação e atividades agrícolas em áreas rurais remotas frequentemente depende de soluções energéticas alternativas, especialmente em locais sem conexão à rede elétrica. Este estudo propõe construir e avaliar, experimentalmente, um sistema de bombeamento acionado por roda d'água flutuante, projetado para operar continuamente em rios com vazão moderada, apresentando-se como alternativa sustentável e de baixo custo, adequada às necessidades de agricultores familiares e comunidades rurais. O sistema foi construído, instalado e testado em um trecho do rio Tormenta, no município de Catanduvas, Estado do Paraná, Brasil, onde foram realizadas medições de vazão bombeada, altura manométrica, torque, velocidade de rotação e velocidade da correnteza. A partir dos dados experimentais, foram determinadas a potência hidráulica, a potência mecânica e a potência de bombeamento, bem como as eficiências hidráulica, mecânica e global do sistema. O protótipo operou de forma contínua, apesar do comportamento intermitente característico da bomba de Wirtz, e alcançou eficiência hidráulica máxima de 72%. As vazões bombeadas mostraram-se compatíveis com as demandas hídricas de pequenas propriedades agrícolas familiares. A análise econômica indicou viabilidade do sistema quando comparado ao custo evitado do abastecimento convencional de água, apresentando tempo de retorno descontado inferior à vida útil estimada do equipamento e custo nivelado de energia próximo de um real por metro cúbico de água bombeada. Os resultados demonstram que rodas de água flutuantes constituem solução sustentável, de baixo custo e tecnicamente viável para comunidades rurais isoladas.

**Palavras-chave:** energia hidrocinética, elevação de água, abastecimento autônomo de água, irrigação alternativa, abastecimento de água renovável

Ref. 304015 – Received 24/01/2026
* Corresponding author - E-mail: marcelo.rotta@unioeste.br
• Accepted 08/06/2026 • Published 27/08/2026
Editors: Ítalo Herbet Lucena Cavalcante & Carlos Alberto Vieira de Azevedo

**Publisher's Note:** The statements, opinions, and data contained in this article are the sole responsibility of the author(s). The Agriambi Journal and/or Editor(s) disclaim any liability for damages to persons or property resulting from any ideas, methods, instructions, or products mentioned in the article.

This is an open-access article distributed under the Creative Commons Attribution 4.0 International License.

## Introduction

Access to water and energy constitutes an essential element for human development and the sustainability of agriculture, especially in rural regions where irrigation is indispensable to ensure productivity. However, millions of people still face restrictions in access to electricity, which limits the adoption of conventional water pumping systems (Herington et al., 2017). In these areas, reliance on fossil fuels to drive pumps or generators is common, a costly and environmentally unfavorable alternative that hinders the modernization of agricultural activities (Ponciano et al., 2020).

The energy sector is responsible for a significant share of global greenhouse gas emissions, reinforcing the need for low-carbon solutions (Sousa et al., 2022). According to Holden et al. (2020), the transition from current energy models requires the reformulation of existing energy matrices, with an emphasis on energy efficiency and the expansion of renewable energy use. This transition must reconcile the satisfaction of human needs, the promotion of social justice, and respect for environmental limits, constituting one of the main contemporary energy and climate challenges (Holden et al., 2021).

Among pumping technologies based on renewable sources, windmills, solar pumps, hydraulic ram pumps, Archimedes screw turbines, and water wheels stand out. Although widely used, these solutions present specific limitations, such as dependence on wind conditions, costs associated with energy storage in solar systems (Khan et al., 2015), or the requirement of a minimum head in the case of hydraulic ram pumps (Luchese, 2020). In this context, systems driven directly by the kinetic energy of rivers offer advantages by operating continuously, with low environmental impact and reduced costs.

Water wheels are among the earliest hydraulic machines developed for the conversion of hydraulic energy into mechanical energy (Quaranta, 2018). Their different configurations—undershot, overshot, breastshot, and stream wheel—allow application under distinct hydraulic conditions (Tevata & Inprasit, 2011). Free-flow water wheels have received increasing attention because they operate directly in the current, without the need for waterfalls or significant civil works (Brandon-Toole et al., 2023). In particular, undershot water wheels are well suited to rural and remote contexts due to their simple construction, low cost, and reduced maintenance requirements (Khan et al., 2015; Sari et al., 2022).

A promising alternative for water pumping in rural areas is the integration of water wheels with the Wirtz pump, a helical device created in 1746, characterized by its simple construction and operation entirely based on renewable energy (Meseret et al., 2024). Its operation is based on the alternating intake of air and water into a helical tube, generating internal pressures capable of lifting the fluid to moderate heights. The hydraulic performance of this system is strongly influenced by geometric and operational variables, such as rotational speed, submergence ratio, number of turns, and external diameter of the spiral—parameters that simultaneously affect flow rate and manometric head, allowing design flexibility according to irrigation needs.

In light of this context, a gap is identified in the literature regarding experimental studies that evaluate, in an integrated manner, the hydraulic performance, efficiency, and economic aspects of systems combining floating water wheels and Wirtz pumps. Thus, this study proposes to construct and experimentally evaluate a pumping system driven by a floating water wheel, designed to operate continuously in rivers with moderate flow, presenting itself as a sustainable, low-cost alternative suited to the needs of family farmers and rural communities.

## Material and Methods

The experimental tests were conducted from February to December 2025 in the district of Ibiracema, located in the municipality of Catanduvas, Paraná state, Brazil, along a reach of the Tormenta River.

The average river depth at the installation point was approximately 0.70 m, measured directly during the testing period. The width of the watercourse was approximately 8.0 m, allowing for the safe installation of the floating structure.

The choice of the site was justified by its proximity to agricultural areas dependent on water pumping and by the need for low-cost solutions for water supply in small rural properties.

The pumping system was designed to operate based on the kinetic energy of the river flow, using a floating water wheel coupled to a Wirtz pump. The water wheel was conceived to be low-cost, simple in construction, and capable of continuous operation without the use of external energy sources.

The support structure was built from carbon steel, with PVC floats and flat aluminum blades, seeking to use easily accessible and low-cost materials in order to meet the criteria for a Minimum Viable Product (MVP). The required float volume was defined based on Archimedes' principle, considering an estimated system mass of 37 kg in the design stage, with a 20% safety margin. The system was equipped with four anchoring points, ensuring stability and proper positioning within the watercourse. The design includes the shaft, bearings, connections, piping, and the spiral winding of the Wirtz pump. The system employs two hose windings arranged in a spiral configuration and connected in series.

Figure 1 presents the design of the pumping system using a floating water wheel, developed using SolidWorks software.

In Figure 1, the water wheel is responsible for converting the hydrokinetic energy of the water current into mechanical energy, and the Wirtz pump is responsible for converting mechanical energy into kinetic pumping energy.

Table 1 presents the main dimensional characteristics of the floating pumping system.

The pumping system was manufactured at the SENAI laboratories in the municipality of Cascavel, state of Paraná, using equipment available at the facility. The instrumentation used in this study aimed to ensure the reliability of the measurements taken during the field tests, allowing for the

**Table 1.** Main characteristics of the components of the floating water wheel pumping system

| Component | Characteristic | Value |
|---|---|---|
| Water wheel | External diameter | 975 mm |
| | Width | 200 mm |
| | Number of blades | 6 |
| | Blade dimensions (height × width) | 186 × 150 mm |
| | Water wheel tube cross-section | 2 × 20 × 20 mm |
| | Structural base (length × width) | 1080 × 804 mm |
| | Base tube cross-section | 2 x 40 × 40 mm |
| Wirtz pump | Hose inner diameter | 12.7 mm |
| | Total hose length | 75 m |
| | Number of turns | 2 |

evaluation of the hydraulic and mechanical performance of the system. The methodology used to perform all the hydrokinetic calculations was based on Çengel & Cimbala (2012).

The rotation of the water wheel was determined by timing the duration and counting the number of complete revolutions over 120-second intervals. Based on these records, the rotation was converted to revolutions per minute (rpm) and remained practically constant throughout the tests (Çengel & Cimbala, 2012).

The flow velocity was determined using the direct method by measuring the time taken for a floating object to travel along a previously marked 5.0 m section. The procedure was repeated five times to reduce the influence of local flow variations (Çengel & Cimbala, 2012).

The pumped flow rate was determined using a container of known volume and a stopwatch. For each manometric head condition, the water discharged through the hose was collected over 180 s, with three consecutive repetitions. From the recorded volumes and times, the average flow rate in liters per minute (L $min^{-1}$) was calculated to ensure greater reliability of the results and was later expressed in cubic meters per second ($m^3$ $s^{-1}$).

The manometric head was adjusted experimentally by raising the discharge hose to the maximum height allowed by site conditions. From this initial height, the hose was gradually lowered in 1.0 m increments. This procedure allowed for evaluating the performance of the system under different hydraulic loads and understanding the relationship between manometric head and pumped flow rate (Çengel & Cimbala, 2012).

In addition, the force exerted by the current on the wheel was measured by applying a load perpendicularly to one of the water wheel blades. This determination was intended to identify the force necessary for the system to reach equilibrium, and enabled the calculation of the torque applied to the shaft, as described in Eq. 1.

$$T = F \times r \quad (1)$$

Where:

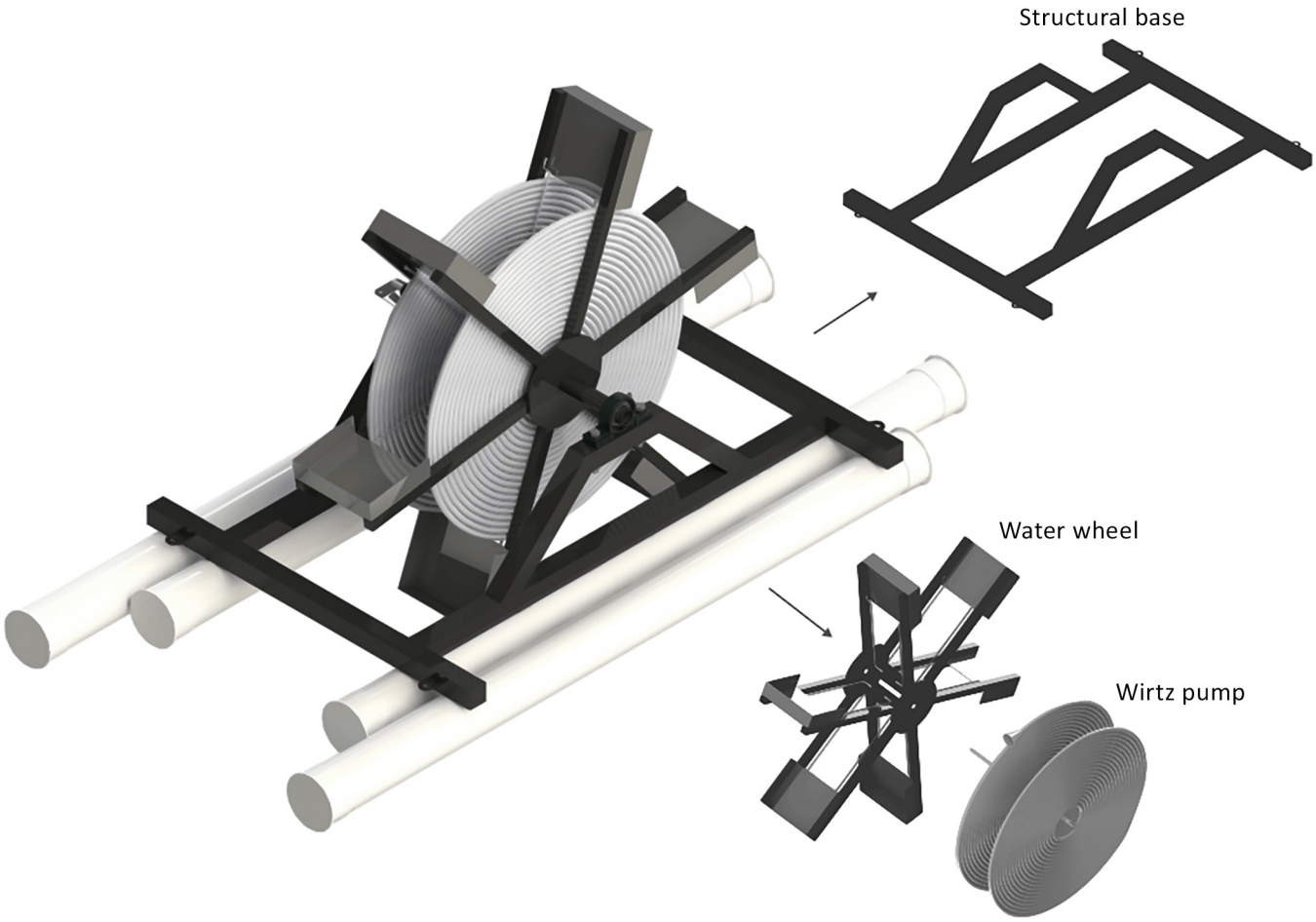


**Figure 1.** Design of the pumping system using a floating water wheel, showing an isometric view and exploded views of the components

T - torque (N m);
F - force exerted on the blades (N); and,
r - water wheel radius (m).

This corresponds to the maximum torque of the system, occurring due to the overlap of the submerged blades, as shown in Figure 2 (Çengel & Cimbala, 2012).

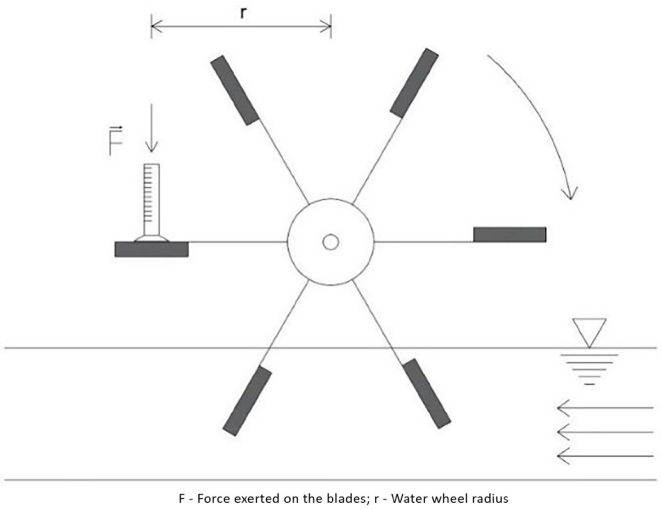


**Figure 2.** Determination of the maximum torque on the floating water wheel using the force exerted by the current

Using the torque and rotation values, it was possible to determine the extracted mechanical power, while the measurements of flow rate and manometric head allowed for the calculation of the pumping power.

The field tests aimed to quantify the hydraulic and mechanical performance of the pumping system driven by the floating water wheel.

The expressions used for the power calculations are based on the classical formulation of fluid mechanics and flow machines, as presented by Çengel & Cimbala (2012).

The hydraulic power available in the flow, considering the predominant kinetic energy, was calculated using Eq. 2.

$$\omega_H = \frac{1}{2}\rho \times A \times V^3 \quad (2)$$

Where:
$\omega_H$ - extracted hydraulic power (W);
$\rho$ - water density (kg m$^{-3}$);
A - submerged blade cross-sectional area (m$^2$); and,
V - flow velocity (m s$^{-1}$).

The mechanical power extracted by the wheel was obtained from the torque and rotation, as shown in Eq. 3.

$$\omega_M = \frac{2\pi \times T \times N}{60} \quad (3)$$

Where:
$\omega_M$ - mechanical power (W);
T - torque (N m); and,
N - water wheel rotation (rpm).

The hydraulic efficiency was obtained using Eq. 4.

$$\eta_H = \frac{\omega_M}{\omega_H} \quad (4)$$

Where:
$\eta_H$ - hydraulic efficiency (-);
$\omega_M$ - mechanical power (W); and,
$\omega_H$ - extracted hydraulic power (W).

The pumping power was calculated using Eq. 5.

$$\omega_B = \rho \times g \times Q \times H_m \quad (5)$$

Where:
$\omega_B$ - pumping power (W);
$\rho$ - water density (kg m$^{-3}$);
g - gravitational acceleration (m s$^{-2}$);
Q - pumped water flow rate (m$^3$ s$^{-1}$); and,
$H_m$ - total manometric head (m).

Based on the measurements taken for different manometric head values and the corresponding average flow rates, the pumping power, mechanical efficiency, and overall efficiency were calculated for each operational condition.

The pumping system operates exclusively with a discharge line, consisting of a hose with an inner diameter of 12.7 mm (1/2″) and a total length of 75 m, in addition to the associated hydraulic singularities. Çengel & Cimbala (2012) provide consolidated equations and information necessary for the calculation of head losses in hydraulic systems.

The total head loss is the sum of distributed and localized losses, as shown in Eq. 6.

$$H_p = hpd + hpl \quad (6)$$

Where:
$H_p$ - total head loss (m);
hpd - distributed head loss (m); and,
hpl - localized head loss (m).

The distributed head loss (hpd) was calculated using the Darcy–Weisbach equation, Eq. 7.

$$hpd = f\frac{L \times V_e^2}{D_i \times 2g} \quad (7)$$

Where:
$D_i$ - internal pipe diameter (m);
$V_e$ - flow velocity (m s$^{-1}$);
L - pipe length (m);
g - gravitational acceleration (m s$^{-2}$); and,
f - friction factor, a function of Re (Reynolds number) and the relative roughness of the pipe $\boldsymbol{\varepsilon}$/D.

Where the friction factor f was defined by the relation 64/Re, valid for laminar flow conditions. This condition was confirmed through the calculation of the Reynolds number for the evaluated flow rates.

Localized losses were determined by summing the k coefficients, as shown in Eq. 8.

$$hpl = \Sigma k \frac{V_e^2}{2g} \quad (8)$$

Table 2 presents the values of the coefficients adopted for calculating localized head losses, according to the hydraulic singularities of the system.

The total head losses were calculated considering the average flow rate obtained in the experimental tests, as well as slightly higher and lower values than this reference, allowing for the characterization of the hydraulic behavior of the system over a representative operating range. The total manometric head ($H_m$) used is expressed by Eq. 9, where $H_g$ is the geometric head.

$$H_m = H_g + H_p \quad (9)$$

The calculated head losses make it possible to construct the system characteristic curve. On the same graph, it is also possible to plot the pump characteristic curve, obtained experimentally. The intersection point of the curves defines the system operating point, corresponding to the balance between the hydraulic energy supplied by the wheel and that required by the discharge line flow.

Experimental data were fitted using simple linear regression in Excel, selecting the trendline with the highest coefficient of determination ($R^2$) using the least-squares method, ensuring a closer match to the actual behavior of the system.

For the assessment of the financial viability of the pumping system driven by a floating water wheel, it was necessary to establish a set of assumptions serving as the basis for the calculations of Net Present Value (NPV), Discounted Payback Period (DPB), and Levelized Cost of Pumped Water (LCOE) (Assaf Neto, 2014; Loth et al., 2022), which are well-established indicators for this type of analysis (Bergmann et al., 2023). The corresponding equations are presented according to Eqs. 10, 11 and 12, respectively.

$$NVP = \sum_{t=1}^{n} \frac{FC_t}{(1+i)^t} - I_0 \quad (10)$$

Where:
NVP - net present value (R$);
$FC_t$ - cash flow in period t (R$);
$I_0$ - initial investment (R$);
i - minimum attractiveness rate (MARR) (decimal);
n - project lifetime (years); and,
t - period (years).

$$DPB = \text{minimun}\{t\}, \text{such that} \sum_{t=1}^{n} \frac{FC_t}{(1+i)^t} \geq -I_0 \quad (11)$$

Where:
DPB - Discounted Payback Period (years).

$$LCOE = \frac{\sum_{t=0}^{n} \frac{It + Mt + Ft}{(1+i)^t}}{\sum_{t=0}^{n} \frac{Et}{(1+i)^t}} \quad (12)$$

Where:
LCOE - levelized cost of pumped water (R$ $m^{-3}$);
It - investment expenses in year t (R$);
Mt - maintenance expenses in year t (R$);
Ft - fuel expenses in year t (R$); and,
Et - energy generated in year t (kWh).

In this study, there is no fuel consumption, consequently Ft can be disregarded in Eq. 12. LCOE was also used to calculate the average cost per cubic meter of water pumped over the lifetime of the equipment.

Table 3 presents the values adopted for the economic analysis calculations in an organized manner.

First, the initial investment was considered, including the acquisition of materials, prototype fabrication, and the services required for assembly and installation. This is a low-cost system, consistent with the initial design concept.

To estimate the annual economic benefit, the cost of water charged by Companhia de Saneamento do Paraná (SANEPAR) was used as a reference, allowing a hypothetical comparison between conventional water supply and water provision through the proposed system. Based on the current tariff structure, a household with a monthly consumption of 30 $m^3$ (a value close to the volume pumped by the experimental system) would have a bill of approximately R$ 242.23, resulting in an annual cost of R$ 2,906.76. This value refers exclusively to water supply, excluding sewage charges, which would increase the bill by about 80%. Although this comparison is not directly applicable to the rural context, it serves as a consistent economic parameter to assess the potential savings provided by the proposed solution.

The analysis also incorporated an annual maintenance cost of R$ 50.00, which covers periodic inspections, adjustments, cleaning, and occasional replacement of simple components. This represents a low cost, around 2% of the initial investment, consistent with the operational simplicity of the floating water wheel.

The Minimum Attractiveness Rate (MARR) used in the calculations was 6% per year (similar to the rate considered for savings accounts), a value commonly employed in feasibility analyses. This rate reflects a conservative estimate of capital return, suitable for low-risk investments with long-term horizons (Assaf Neto, 2014).

The adopted lifetime of the system was 10 years, considering the expected behavior of the materials used and the low operational complexity of the assembly. For the LCOE calculation, an annual pumped volume of 388.94 $m^3$ was considered, estimated based on the capacity observed experimentally.

These assumptions allow for a robust economic analysis, consistent with the experimental nature of the system and aligned with the actual conditions of isolated rural properties not connected to the electrical grid, with small nearby water flows. Moreover, they enable a transparent quantification of the potential savings associated with the use of the floating water wheel compared to conventional water supply alternatives.

**Table 2.** Hydraulic singularities and their localized loss coefficients (k)

| Singularity | k |
|---|---|
| 90° short-radius elbow (2 units) | 1.6 |
| Quick coupling | 1 |
| 1/2″ to 3/4″ threaded adapter | 0.3 |
| 1/2″ to 1/2″ connector | 0.2 |

## Results and Discussion

The experimental tests enabled the characterization of the performance of the floating water wheel and its interaction with the Wirtz pump coupled to the system. The pumped flow rates ranged from 0.48 to 0.90 L $min^{-1}$, depending on the applied manometric head, which was initially set at 8.42 m and gradually reduced to 2.42 m. The low observed flow rates, associated with relatively high manometric heads, can be attributed to the influence of the tube diameter on system performance. As discussed by Millimouno & Cooke (2024), using smaller diameter tubes allows a greater number of coils to be wrapped around the wheel, favoring higher manometric heads, albeit with reduced volumetric discharge.

During operation, blade overlap was observed, a phenomenon that produces periodic oscillations in both the effectively submerged area and the hydrodynamic force exerted by the current. At certain moments, only one blade is submerged, while at others, two blades act simultaneously, resulting in a sinusoidal cyclic behavior. At some points, the system presents an increased area and higher force, whereas at others, only a single blade is active, resulting in a temporary reduction in available torque. Based on this observation, the average submerged blade area during each rotation cycle was calculated, resulting in a value of 0.04185 $m^2$.

The calculations of hydraulic power and torque were adjusted based on effective average values, in order to more accurately represent the power actually transferred to the system over time. The average current velocity was determined to be 0.866 m $s^{-1}$, while the load required to maintain the assembly in equilibrium was 1.627 kg. From this load, and considering the operating conditions, an average torque per rotation cycle of 7.182 N m was obtained.

The hydraulic power available ($\omega_H$) in the water wheel was calculated as 13.59 W, considering the interaction of the current with the average submerged area of the blades. Based on the experimentally measured torque and the corresponding average rotation of 13 rpm, a mechanical power of 9.78 W ($\omega_M$) transmitted to the shaft was obtained. Thus, the hydraulic efficiency of the assembly reached 72.01%, demonstrating a significant utilization of the available hydrokinetic energy, particularly considering that this is a small-scale system operating in free flow. The maximum mechanical and overall efficiencies were 7.94 and 5.71%, respectively. This hydraulic efficiency is consistent with the results presented by Sule et al. (2020) and Teoh et al. (2022), who highlighted the high efficiency achieved in six-bladed water wheels subjected to natural flows. The calculated mechanical and overall efficiencies of the system are shown in Table 4.

Table 4 presents the experimentally obtained head and flow rate values, as well as the corresponding calculated pumping power and mechanical and overall efficiencies.

These results were consistent with the trends described by Adanta et al. (2020), who demonstrated that the number of blades simultaneously influences torque, efficiency, and rotational speed. Although a higher number of blades can theoretically increase efficiency, configurations with fewer blades tend to exhibit greater stability and rotational speed—desirable characteristics in small-scale, low-cost systems such as the prototype developed in this study.

A widely documented aspect in the literature, and confirmed experimentally, is the strong dependence of hydraulic power on current velocity (Çengel & Cimbala, 2012; Kumar et al., 2020). Since the available power is directly associated with the term $V^3$ (current velocity), small fluctuations in river speed can cause significant increases or decreases in the kinetic power available to drive the wheel.

In this context, the results presented by Kumar et al. (2020) confirm this relationship, showing that flow velocity directly influences the pumped flow rate. The authors observed that an increase in water velocity in the channel significantly increases discharge, as it enhances the kinetic energy transferred to the wheel and intensifies the pumping process, as demonstrated in this study.

The results indicate that, although the system exhibits high hydraulic efficiency, the mechanical and overall efficiencies presented small values (less than 10%) — a behavior expected in devices driven predominantly by the kinetic energy of the current. In the specific case of the Wirtz pump, this condition is further accentuated because the pumping occurs intermittently, involving not only water but also air volumes responsible for internal pressurization, which are not accounted for in the calculation of useful flow rate.

Furthermore, it was observed that an increase in the manometric head leads to a reduction in the pumped flow rate, while slightly increasing mechanical efficiency. This relationship suggests the existence of a more favorable operational range between approximately 6 and 7 m, where the system demonstrated the most balanced combination of hydraulic, mechanical, and overall performance.

Under the observed operating conditions, the flow within the spiral remained predominantly laminar, a characteristic associated with the low flow rates obtained and, consequently, the reduced internal velocities along the tubing.

**Table 3.** Assumptions adopted for the economic analysis of the system

| Parameter | Value | Description |
|---|---|---|
| Initial investment | R$ 2,500.00 | Total cost of the prototype and associated services |
| Annual avoided cost | R$ 2,906.76 | Annual cost of water paid to SANEPAR, corresponding to urban consumption of 360 $m^3$ per year |
| Annual maintenance | R$ 50.00 | Estimated annual cost for simple system maintenance |
| Minimum Attractiveness Rate (MARR) | 6% per year | Rate used to discount future cash flows |
| Considered lifetime | 10 years | Estimated lifetime for economic analysis purposes |

Based on the experimental data, the pump characteristic curve was constructed, showing the inverse relationship between flow rate and manometric head—a behavior widely reported in the literature for pumping systems. From the calculations of distributed and localized head losses, the system characteristic curve was also developed. Both curves are shown in Figure 3.

In Figure 3, for the design of the system curve, a geometric height of 5 m was initially considered, and from flow rate values established in the range of 0.2 to 1.4 L $min^{-1}$, the head losses, and consequently the manometric heads of the system, were calculated. For the design of the pumping curve, the collected values of manometric head and pumping flow rate, as presented in Table 4, were used. The curve that best fit the collected data was calculated, and its equation is presented in Figure 3.

During the experimental tests, it was observed that the flow rate values did not follow a strictly decreasing trend with increasing manometric head (as shown in Table 4), as would be expected in conventional pumps. In some cases, higher flows were recorded at higher heads, a behavior that at first glance appears counterintuitive.

This phenomenon is associated with the specific characteristics of the system under study: the Wirtz pump operates intermittently, alternating the pumping of water and air, resulting in pulsating, non-steady cycles. Additionally, small variations in the position of the floating structure continuously influence the available power. Since measurements were taken over relatively short intervals, these instantaneous fluctuations can artificially increase the recorded flow at certain heads, particularly when coinciding with periods of stronger pulses.

Thus, the small inversions observed between manometric head and flow rate do not indicate anomalous hydraulic behavior, but rather reflect the pulsating nature and cycle-dependent operation of the Wirtz pump in a natural environment, highlighting the dynamic character of the system.

In Figure 3 of the pumping system, the operating point was determined by the intersection of the pump curve with the system curve, constructed from distributed losses (Darcy–Weisbach) and localized losses (sum of k coefficients). The curve showed that, although the system operates at low flow rates, it can safely operate at considerable manometric heads.

During the experimental tests, it was observed that the immersion depth of the blades exhibited minor variations throughout the wheel movement. These oscillations were mainly due to the natural behavior of the flow and the movement of the floating structure. Although noticeable, these variations were not directly incorporated into the calculations, as their influence on the submerged area is small and modeling them would require a complex transient flow analysis.

The system demonstrated a discounted payback period of 11 months, indicating a rapid recovery of the initial investment. This performance was also reflected in the Net Present Value, which reached R$ 18,526.00 at the end of the analysis horizon. This result shows that the system not only pays back in a short period but also generates a significant accumulated economic return over its useful life.

LCOE, expressed in R$ $m^{-3}$, is appropriate and consistent with the nature of the system. With no electricity or fuel costs and minimal operational expenses, the obtained value of R$ 1.00 $m^{-3}$ highlights economically relevant performance, especially for isolated rural properties that require low-cost water supply solutions.

The results demonstrate that the floating waterwheel pumping system is financially viable, technically efficient, and has significant socio-environmental potential as an alternative for water pumping in isolated rural communities with small water streams. The floating water wheel developed in this study could serve a rural property with an average daily consumption of 1000 L of water, and could be used for the family's own consumption or for a localized sprinkler irrigation system. The absence of energy costs, combined with the low initial investment, enables a rapid payback period and significant savings over the service life of the system. These factors consolidate the floating waterwheel system as a low-cost, sustainable, and accessible solution for small farmers and remote properties.

The findings support the observations of Hashmi et al. (2022), highlighting that hydraulic energy is characterized by low operational cost and high efficiency, directly aligning it with the Sustainable Development Goals (SDGs), particularly Goal 7, which aims to expand universal access to clean, safe, and economically accessible energy.

**Table 4.** Manometric head, pumped flow rate, pumping power and mechanical and overall efficiencies of the system

| | Manometric head – $H_m$ (m) | | | | | | |
|---|---|---|---|---|---|---|---|
| | 8.42 | 7.42 | 6.42 | 5.42 | 4.42 | 3.42 | 2.42 |
| (Q) Flow rate (L $min^{-1}$) | 0.48 | 0.64 | 0.63 | 0.74 | 0.85 | 0.79 | 0.90 |
| (Q) Flow rate ($m^3$ $s^{-1}$) ($\times 10^{-5}$) | 0.80 | 1.07 | 1.05 | 1.23 | 1.42 | 1.32 | 1.50 |
| ($\omega_B$) Pumping power (W) | 0.66 | 0.78 | 0.66 | 0.66 | 0.62 | 0.44 | 0.36 |
| ($\eta_M = \omega_B/\omega_M$) Mechanical efficiency (%) | 6.77 | 7.94 | 6.75 | 6.70 | 6.31 | 4.50 | 3.63 |
| ($\eta_G = \omega_B/\omega_H$) Overall efficiency (%) | 4.87 | 5.71 | 4.86 | 4.83 | 4.54 | 3.24 | 2.61 |

$H_m$ - is the manometric head; Q - is the pumped flow rate; ωH, ωM, and ωB - correspond to hydraulic power, mechanical power, and pumping power, respectively. ωH = 13.59 W, as calculated by Eq. 2 (assuming 1000 kg $m^{-3}$ for the water density, 0.04185 $m^2$ for the average submerged blade area and 0.866 m $s^{-1}$ for the average water current velocity); ωM = 9.78 W, as calculated by Eq. 3 (assuming 7.182 N m for the average torque per rotation cycle and 13 rpm for the average rotation of the water wheel) and ωB - Variable values, as calculated by Eq. 5 (assuming 9.81 m $s^{-2}$ for the gravity acceleration). The flow rates presented in L $min^{-1}$ correspond, respectively, to $8.0\times10^{-6}$, $1.07\times10^{-5}$, $1.05\times10^{-5}$, $1.23\times10^{-5}$, $1.42\times10^{-5}$, $1.32\times10^{-5}$, and $1.50\times10^{-5}$ $m^3$ $s^{-1}$, obtained by direct conversion to International System Units

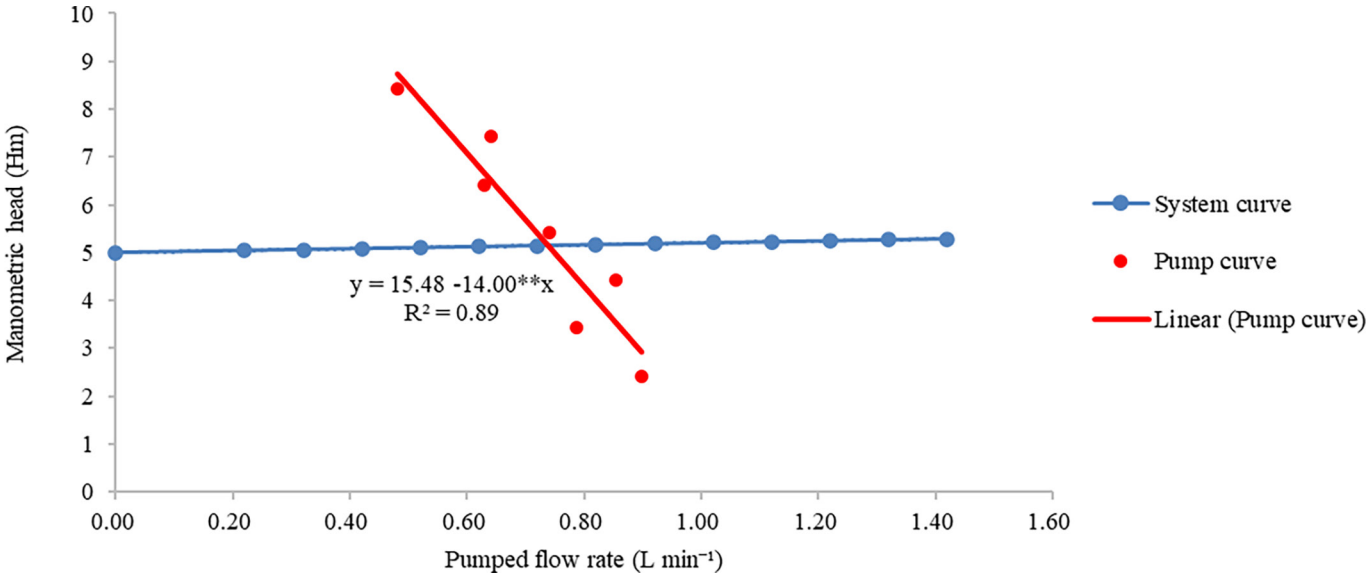


** - Significant at p ≤ 0.01 according to F-test

**Figure 3.** System curve (or installation curve), pump characteristic curve, and operating point (intersection between the curves) for the manometric head

## Conclusions

1. The pumped flow rates ranged from 0.48 to 0.90 L min$^{-1}$ for manometric heads between 8.42 and 2.42 m. The calculated values for hydraulic power ($\omega_H$) and mechanical power ($\omega_M$.) were 13.59 and 9.78 W, respectively.

2. The hydraulic efficiency of the system reached 72.01%, indicating good utilization of the hydrokinetic energy available in the current.

3. The Levelized Cost of pumped water was approximately R$ 1.00 per cubic meter over the analyzed service life. The Net Present Value was R$ 18,526.00, and the Discounted Payback period was 11 months.

**Contribution of authors:** Preparation of the article and literature review: Marcelo P. Rotta; Research design and supervision of the work: Marcelo P. Rotta, Carlos E. C. Nogueira, Jair A. C. Siqueira, Eloy L. de Mello and Marcio A. V. Boas; Administration and funding acquisition: Marcelo P. Rotta, Carlos E. C and Samuel N. M. de Souza.

**Data Availability Statement:** The authors declare that there are no data underlying the text.

**Conflict of Interest:** The authors declare that they have no conflicts of interest.

**Financing statement:** This study was financed in part by the Coordenação de Aperfeiçoamento de Pessoal de Nível Superior - Brazil (CAPES) - Finance Code 001.

**Acknowledgments:** The authors would like to thank the Programa de Pós-Graduação em Engenharia de Energia na Agricultura and CAPES for their support.

## Literature Cited

Adanta, D. et al. Effect of the number of blades on undershot waterwheel performance for straight blades. IOP Conference Series: Earth and Environmental Science, v.431, 012024, 2020. https://doi.org/10.1088/1755-1315/431/1/012024

Assaf Neto, A. Finanças corporativas e valor. 7.ed. São Paulo: Editora Atlas, 2014. 824p.

Bergmann, B. H. et al. Estudo da combinação de indicadores para análise da viabilidade de projetos: uma revisão de literatura. Revista GeSec, v.14, p.10644-10665, 2023. https://doi.org/10.7769/gesec.v14i6.2397

Brandon-Toole, M. et al. The effect of blade depth ratio on the performance of in-stream water wheels. Energy for Sustainable Development, v.77, 101346, 2023. https://doi.org/10.1016/j.esd.2023.101346

Çengel, Y. A.; Cimbala, J. M. Mecânica dos fluidos: Fundamentos e Aplicações. Porto Alegre: AMGH, 2012. 277p.

Hashmi, A. et al. Revisiting the Indus Basin model for an energy sustainable Pakistan. Water, v.14, 702, 2022. https://doi.org/10.3390/w14050702

Herington, M. J. et al. Rural energy planning remains out-of-step with contemporary paradigms of energy access and development. Renewable and Sustainable Energy Reviews, v.67, p.1412–1419, 2017. http://dx.doi.org/10.1016/j.rser.2016.09.103

Holden, E. et al. Grand narratives for sustainable mobility: a conceptual review. Energy Research & Social Science, v.65, 101454, 2020. https://doi.org/10.1016/j.erss.2020.101454

Holden, E. et al. A review of dominant sustainable energy narratives. Renewable and Sustainable Energy Reviews, v.144, 110955, 2021. https://doi.org/10.1016/j.rser.2021.110955

Khan, F. U. et al. Modeling, simulation and fabrication of an undershot floating waterwheel. Journal of Engineering and Applied Sciences, v.34, p.55-69, 2015.

Kumar, F. et al. Development and testing of a spiral type water wheel pumping system. International Journal of Current Microbiology and Applied Sciences, v.9, p.3061–3069, 2020. https://doi.org/10.20546/ijcmas.2020.905.364

Loth, E. et al. Why we must move beyond LCOE for renewable energy design. Advances in Applied Energy, v.8, 100112, 2022. https://doi.org/10.1016/j.adapen.2022.100112

Luchese, T. C. Considerações teóricas a respeito de um carneiro hidráulico sob condições ideais de funcionamento. Brazilian Journal of Development, v.6, p.46766–46787, 2020. https://doi.org/10.34117/bjdv6n7-349

Meseret, M. et al. Experimental study on the parameters affecting the performance of spiral tube pump. Scientific Reports, v.14, 22425, 2024. https://doi.org/10.1038/s41598-024-73234-w

Millimouno, A.; Cooke, R. A. Design, construction, and field testing of a spiral water wheel pump. African Journal of Food, Agriculture, Nutrition and Development, v.24, p.25990–26006, 2024. https://doi.org/10.18697/ajfand.129.24215

Ponciano, I. M. et al. Are water wheels a rural cost-effective energy technology? Inovação & Sociedade, v.1, p.1-16, 2020.

Quaranta, E. Stream water wheels as renewable energy supply in flowing water: theoretical considerations, performance assessment and design recommendations. Energy for Sustainable Development, v.45, p.96–109, 2018. https://doi.org/10.1016/j.esd.2018.05.002

Sari, D. P. et al. Performance of undershot waterwheel in pico scale with difference in the blades number. Journal of the Brazilian Society of Mechanical Sciences and Engineering, v.44, 107, 2022. https://doi.org/10.1007/s40430-022-03430-0

Sousa, S. et al. Energy efficiency legislation in Brazil towards net zero emissions: projections and propositions for São Paulo State. Revista Brasileira de Energia, v.28, p.31–47, 2022. https://doi.org/10.47168/rbe.v28i4.768

Sule, L. et al. Performance of undershot water wheel with bowl-shaped blades model. International Journal of Technology, v.11, p.278–287, 2020. https://doi.org/10.14716/ijtech.v11i2.2465

Teoh, S. K. et al. Investigation of design parameters on self-floating water wheel for micro-hydropower generation. International Journal of Green Energy, v.19, p.931–940, 2022. https://doi.org/10.1080/15435075.2021.1975123

Tevata, A.; Inprasit, C. The effect of paddle number and immersed radius ratio on water wheel performance. Energy Procedia, v.9, p.359–365, 2011. https://doi.org/10.1016/j.egypro.2011.09.039